

Renal Cell Carcinoma: Role of MR Imaging in the Assessment of Muscular Venous Branch Invasion¹

Christoph A. Karlo, MD
Pier Luigi Di Paolo, MD
Olivio F. Donati, MD
Paul Russo, MD
Satish Tickoo, MD
Hedvig Hricak, MD, PhD, Dr(hc)
Oguz Akin, MD

Purpose:

To assess diagnostic performance and interreader agreement of tumor-to-sinus distance measurements and visual assessment of renal sinus fat invasion at T2-weighted magnetic resonance (MR) imaging as predictors of muscular venous branch invasion (MVBI) in patients with renal cell carcinoma (RCC).

Materials and Methods:

The institutional review board approved this retrospective study and waived the informed consent requirement. The study was HIPAA compliant. A total of 186 consecutive patients underwent preoperative 1.5-T MR imaging; 188 RCCs were identified. Blinded to histopathologic information, two readers independently measured the tumor-to-sinus distance and assessed renal sinus fat invasion on transverse and coronal T2-weighted MR images. Interreader agreement (intraclass correlation coefficient, Cohen κ) and performance characteristics of imaging tests were calculated. Histopathologic findings served as the standard of reference.

Results:

Histopathologic findings indicated MVBI in 35% (66 of 188) of tumors. At imaging, all tumors with MVBI had a tumor-to-sinus distance of 0 mm. All tumors with renal sinus fat invasion at imaging had MVBI. Sensitivity and specificity for the detection of renal sinus fat invasion were 100% (95% confidence interval [CI]: 92%, 100%) and 94% (95% CI: 89%, 98%). In the absence of renal sinus fat invasion at imaging, a tumor-to-sinus distance of 0 mm was associated with MVBI in 21% (18 of 86) of cases. Interreader agreement for quantitative (intraclass correlation coefficient = 0.92; 95% CI: 0.89, 0.94) and qualitative (κ = 0.89; 95% CI: 0.81, 0.96) assessments was excellent.

Conclusion:

Tumor-to-sinus distance measurements and the assessment of renal sinus fat invasion at T2-weighted MR imaging can be used reliably to rule out MVBI in patients with RCC.

©RSNA, 2013

¹From the Departments of Radiology (C.A.K., P.L.D.P., O.F.D., H.H., O.A.), Urology (P.R.), and Pathology (S.T.), Memorial Sloan-Kettering Cancer Center, 1275 York Ave, Radiology Academic Offices, Room C278, New York, NY 10065. Received July 16, 2012; revision requested August 29; revision received August 31; accepted October 2; final version accepted November 9. C.A.K. and O.F.D. supported by the Swiss National Science Foundation. **Address correspondence to C.A.K.**

Invasion of the renal sinus fat in patients with renal cell carcinoma (RCC) is an important surgical pathologic finding that affects tumor staging and patient prognosis (1–3). However, before invading the renal sinus fat, RCCs extend into muscular venous branches of the renal vein, which then serve as the main pathways for renal sinus fat invasion (4–7). Muscular venous branches of the renal vein emerge from interlobar veins at the interface between the renal parenchyma and renal sinus and continue their course through the adipose tissue of the renal sinus to form the main renal vein after three or four anastomoses (5).

In patients with RCC, muscular venous branch invasion (MVBI) is considered a key criterion for tumor staging and an important adverse prognostic factor regarding recurrence-free and overall survival (8,9). Moreover, the effect of MVBI on patient prognosis is comparable with that of main renal vein invasion or inferior vena cava invasion (9). Thus, the ability to assess

the presence of MVBI preoperatively in patients with RCC would be of considerable clinical value.

To date, to our knowledge, there have been no studies to investigate the role of cross-sectional imaging in the assessment of MVBI. Although magnetic resonance (MR) imaging is useful for staging RCC (10), its spatial resolution may not be sufficient to allow direct visualization of the muscular venous branches of the renal vein, some of which have calibers of less than 2 mm (5). However, we hypothesize that the shortest distance between the renal tumor and the adipose tissue of the renal sinus, as well as evidence of renal sinus fat invasion at imaging, may serve as surrogate predictors of MVBI in patients with RCC.

Thus, the objective of our study was to assess diagnostic performance characteristics and interreader agreement of tumor-to-sinus distance measurements and the qualitative assessment of renal sinus fat invasion on transverse and coronal T2-weighted MR images as predictors of MVBI in patients with RCC, with use of histopathologic examination as the standard of reference.

Advances in Knowledge

- A tumor-to-sinus distance greater than 0 mm at imaging was used to rule out muscular venous branch invasion (MVBI) in renal cell carcinoma (RCC) in 100% (49 of 49) of cases.
- When renal sinus fat invasion was present at imaging, MVBI was identified in 100% (48 of 48) of cases at histopathologic examination.
- When renal sinus fat invasion was absent at imaging and the tumor-to-sinus distance was 0 mm, MVBI was identified in 21% (18 of 86) of cases at histopathologic examination.
- Interreader agreement was excellent for tumor-to-sinus distance measurements (intraclass correlation coefficient = 0.92; 95% confidence interval [CI]: 0.89, 0.94) and the visual assessment of renal sinus fat invasion (κ = 0.89; 95% CI: 0.81, 0.96).

Materials and Methods

Patients

The institutional review board approved this retrospective study and waived the informed consent requirement. The study was compliant with the Health Insurance Portability and Accountability Act.

The inclusion criteria for our study were (a) total or partial nephrectomy performed at our institution during the

Implication for Patient Care

- Tumor-to-sinus distance measurements and visual assessment of renal sinus fat invasion at MR imaging are useful surrogate markers for assessing MVBI, a TNM stage-defining histopathologic finding that substantially affects the prognosis and treatment of patients with RCC.

period from January 2005 to July 2011; (b) preoperative 1.5-T MR imaging of the abdomen, including transverse and coronal T2-weighted sequences, performed within 90 days before surgery (median time, 28.5 days; range, 1–90 days) and available in Digital Imaging and Communications in Medicine format through the hospital's picture archiving and communication system; (c) the use of surgical pathologic examination results to confirm the diagnosis of RCC, establish Fuhrman grade in case of clear cell carcinoma, and confirm the presence or absence of MVBI by tumor.

As shown in the patient selection flowchart in Figure 1, 186 patients were eligible for the study. The patients' demographic and tumor characteristics are summarized in Table 1.


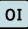
MR Imaging Technique

MR imaging studies were performed with 1.5-T units (Signa Excite or Genesis Signa, GE Medical Systems, Milwaukee, Wis [n = 164]; Avanto, Espree, or Symphony, Siemens Medical Solutions, Forchheim, Germany [n = 23]; or Infineon, Philips Medical Systems, Eindhoven, the Netherlands [n = 1]). Relevant parameters regarding the transverse and coronal T2-weighted sequences are summarized in Table 2.

MR Image Analysis

Without access to histopathologic information, two radiologists with more

Published online before print

10.1148/radiol.13121555 Content codes:  

Radiology 2013; 267:454–459

Abbreviations:

CI = confidence interval
MVBI = muscular venous branch invasion
RCC = renal cell carcinoma

Author contributions:

Guarantors of integrity of entire study, C.A.K., O.A.; study concepts/study design or data acquisition or data analysis/interpretation, all authors; manuscript drafting or manuscript revision for important intellectual content, all authors; manuscript final version approval, all authors; literature research, C.A.K., P.L.D.P., S.T., O.A.; clinical studies, C.A.K., P.L.D.P., S.T., O.A.; experimental studies, P.R., statistical analysis, C.A.K.; and manuscript editing, all authors

Conflicts of interest are listed at the end of this article.

Table 1

Patient and Tumor Characteristics	
Characteristic	Datum
Sex	
Male	67 (124/186)
Female	33 (62/186)
Age (y)*	
Male	59 (34–83)
Female	56 (17–84)
Type of RCC†	
Clear cell	76 (143/188)
Chromophobe	12 (22/188)
Papillary	11 (21/188)
Unclassified	1 (2/188)
Tumor size (cm)**	5.3 (1.3–23.0)
Tumor side†	
Right	51 (96/188)
Left	49 (92/188)
Tumor stage of RCC†	
pT1a	35.6 (67/188)
pT1b	14.4 (27/188)
pT2a	5.3 (10/188)
pT2b	5.3 (10/188)
pT3a	12.2 (23/188)
pT3b	26.6 (50/188)
pT4	0.5 (1/188)
Fuhrman nuclear grade‡	
1	2 (3/143)
2	43 (62/143)
3	37 (53/143)
4	17 (25/143)

Note.—Except where otherwise indicated, data are percentages, with raw data in parentheses. Percentages may not add up to 100% owing to rounding.

* Data are medians, with ranges in parentheses.

† In terms of the histopathologic data, tumor stage was determined according to the sixth edition of the American Joint Committee on Cancer cancer staging manual (11) for all tumor types except angiomyolipoma.

‡ For clear cell RCCs only.

Table 2

MR Imaging Parameters		
Parameter	Transverse Plane	Coronal Plane
Repetition time (msec)	921–4300	850–6000
Echo time (msec)	80.9–200	64.0–122
Field of view	Fitted to patient	Fitted to patient
Section thickness (mm)	4–8	4–8
No. of phase-encoding steps	176–384	192–512
No. of frequency steps	256–512	256–512
No. of signals acquired	0.5–3	0.5–3

Figure 1

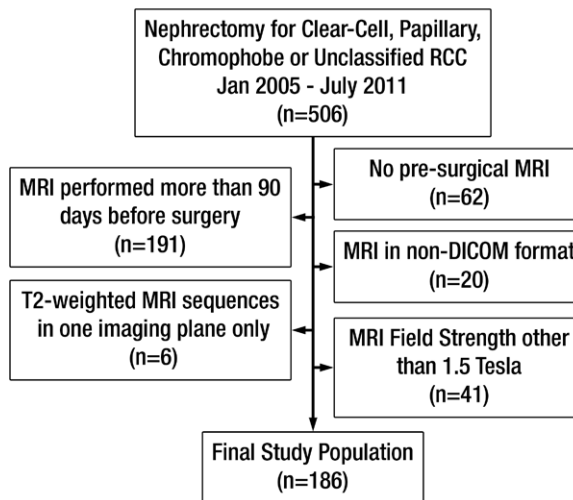


Figure 1: Flowchart of patient selection. *DICOM* = Digital Imaging and Communications in Medicine, *MRI* = MR imaging.

than 5 (C.A.K. [reader 1]) and more than 3 (P.L.D.P. [reader 2]) years of experience interpreting genitourinary imaging studies independently reviewed all MR images by using picture archiving and communication system software (Centricity; GE Medical Systems). First, both readers qualitatively assessed the transverse and coronal T2-weighted MR images for the presence or absence of renal sinus fat invasion by tumor. Then, each reader measured the shortest distance in millimeters between the tumor margin

closest to the adipose tissue of the renal sinus and the interface between the renal parenchyma and renal sinus, henceforth referred to as the tumor-to-sinus distance. The shortest tumor-to-sinus distance in the transverse plane and the shortest tumor-to-sinus distance in the coronal plane were recorded (Figs 2, 3).

Standard of Reference

Original surgical histopathologic reports served as the standard of reference for the presence or absence of MVBI, as well as the presence or absence of renal sinus fat invasion. At surgical histopathologic examination, tumor types were classified as clear cell, papillary, chromophobe, or unclassified RCC. In addition, each clear cell carcinoma was classified according to the Fuhrman

classification system by a genitourinary pathologist (S.T.) with more than 20 years of experience (12).

Statistical Methods

To assess interreader agreement regarding the tumor-to-sinus distance measurements, we calculated the intraclass correlation coefficient for absolute agreement, including the corresponding 95% confidence intervals (CIs) (13). To assess interreader agreement regarding the assessment of renal sinus fat invasion, we calculated Cohen κ values, including the corresponding 95% CIs.

A Pearson correlation coefficient was used to correlate tumor-to-sinus distance measurements obtained from the transverse and coronal imaging planes. A Spearman rank correlation

Figure 2

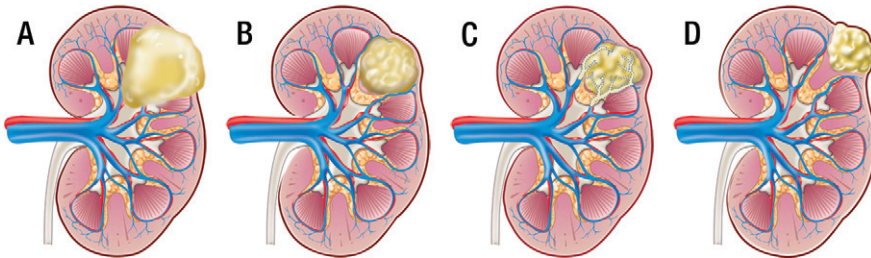


Figure 2: Illustration shows examples in which RCC, *A*, extensively invades the renal sinus, *B*, abuts the renal sinus, *C*, abuts the renal sinus and invades muscular venous branches of the renal vein, and, *D*, is separate from the renal sinus.

Figure 3

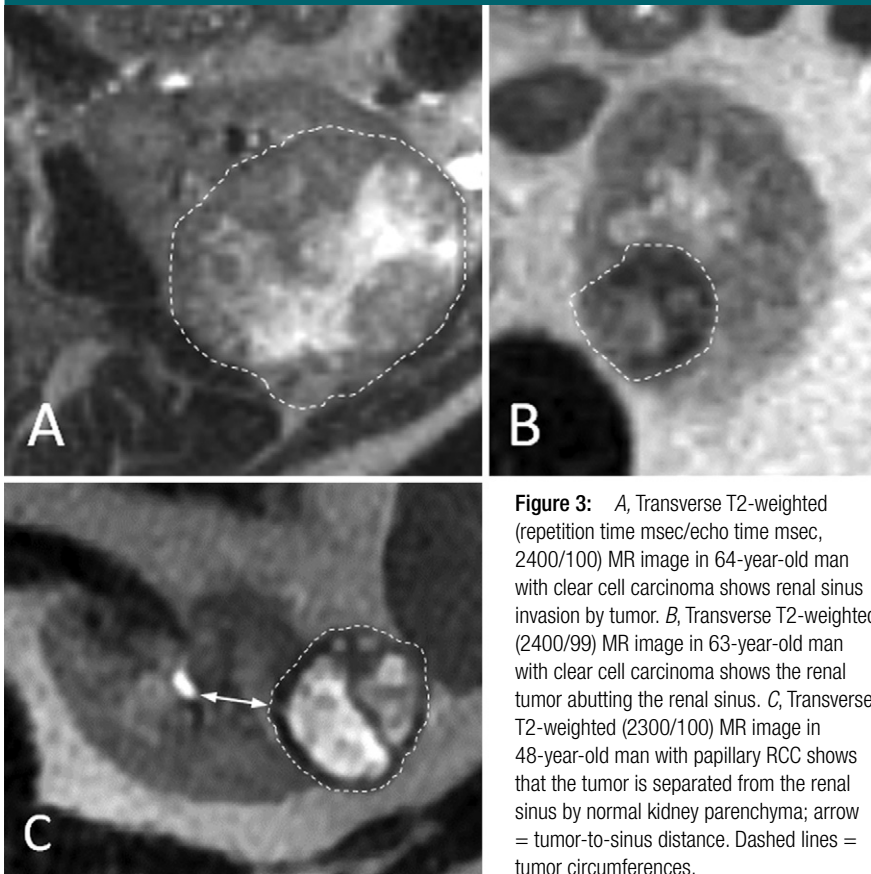


Figure 3: *A*, Transverse T2-weighted (repetition time msec/echo time msec, 2400/100) MR image in 64-year-old man with clear cell carcinoma shows renal sinus invasion by tumor. *B*, Transverse T2-weighted (2400/99) MR image in 63-year-old man with clear cell carcinoma shows the renal tumor abutting the renal sinus. *C*, Transverse T2-weighted (2300/100) MR image in 48-year-old man with papillary RCC shows that the tumor is separated from the renal sinus by normal kidney parenchyma; arrow = tumor-to-sinus distance. Dashed lines = tumor circumferences.

coefficient was used to correlate between the presence of MVBI and Fuhrman grades of clear cell carcinoma, which were consolidated into low grade (ie, grades 1 and 2) and high grade (ie, grades 3 and 4), as previously suggested (14). The

Kruskal-Wallis test was used to test for significant differences in histopathologic tumor size between tumors with MVBI and tumors without MVBI, significant differences in tumor-to-sinus distance between tumors with MVBI and tumors without MVBI, and

significant differences in the frequency of MVBI between low-grade and high-grade clear cell carcinoma.

Sensitivity, specificity, negative predictive value, and positive predictive value for the identification of MVBI in case the tumor-to-sinus distance was 0 mm in patients without evidence of renal sinus fat invasion at imaging were assessed by using χ^2 tests of contingency. Sensitivity, specificity, negative predictive value, and positive predictive value for the identification of renal sinus fat invasion at imaging were also assessed by using χ^2 tests of contingency.

Two-sided *P* values of less than .05 were considered to indicate statistically significant differences. All statistical analyses were performed by using commercially available software (SPSS, version 19; IBM, Armonk, NY).

Results

Histopathologic Findings

In the 186 patients, a total of 188 RCCs were detected by means of histopathologic examination (Table 1). Two patients had more than one carcinoma (one had two clear cell carcinomas in the same kidney, and one had one clear cell and one chromophobe carcinoma in the same kidney). MVBI was present in 35.1% (66 of 188) of RCCs. MVBI was more common in clear cell (81.8% [54 of 66]) than in chromophobe (16.7% [11 of 66]) and unclassified (1.5% [one of 66]) RCCs. Renal sinus fat invasion was present in 21.3% (40 of 188) of carcinomas and was more common in clear cell (72.5% [29 of 40]) than in chromophobe (25% [10 of 40]) and unclassified (2.5% [one of 40]) RCCs.

All patients with renal sinus fat invasion had MVBI (21.3% [40 of 188]). However, in 39% (26 of 66) of cases with MVBI, renal sinus fat invasion was absent. RCCs were significantly larger in cases with MVBI (median, 9.0 cm; range, 3.2–20.5 cm) than in cases without MVBI (median, 3.6 cm; range, 1.3–23.0 cm; *P* < .001). The presence of MVBI was associated with high-grade clear cell carcinoma ($\rho = 0.4$, *P* < .01);

MVBI was identified significantly more often in high-grade (78% [43 of 55]) than in low-grade (22% [12 of 55], $P < .001$) clear cell carcinomas.

Interreader Agreement

Interreader agreement regarding all tumor-to-sinus distance measurements (intraclass correlation coefficient = 0.92; 95% CI: 0.89, 0.94) was excellent. Interreader agreement regarding the assessment of renal sinus fat invasion ($\kappa = 0.89$; 95% CI: 0.81, 0.96) was also excellent.

Renal Sinus Fat Invasion

At imaging, both readers detected renal sinus fat invasion in 25.5% (48 of 188) of cases. All cases that were positive for renal sinus fat invasion at histopathologic examination (40 of 188) were identified correctly at imaging by both readers. For both readers, sensitivity, specificity, negative predictive value, and positive predictive value for the detection of renal sinus fat invasion at imaging were 100% (95% CI: 91%, 100%), 94% (95% CI: 89%, 97%), 100% (95% CI: 97%, 100%), and 83% (95% CI: 70%, 92%), respectively (40 true-positive, eight false-positive, 135 true-negative, and no false-negative findings).

Tumor-to-Sinus Distance

At imaging, both readers measured the tumor-to-sinus distance on transverse T2-weighted MR images in 91.5% (172 of 188) of tumors and on coronal T2-weighted MR images in 84.6% (159 of 188) of tumors. In 2.7% (five of 188) of tumors, both readers determined that the tumor-to-sinus distance measurement was possible on neither the transverse nor the coronal MR images because the renal tumor was located on either the very anterior or the very posterior aspect of the upper or lower kidney pole and, therefore, the tumor and the renal sinus were never visible on the same image. These five tumors were excluded from further analysis, which thus consisted of 97% (183 of 188) of tumors.

A moderate positive correlation was found between tumor-to-sinus distance

measurements obtained from the transverse and coronal imaging planes for both readers (reader 1, $r = 0.63$; reader 2, $r = 0.53$; both, $P < .001$). For the tumor-to-sinus distance analysis, we used the shortest tumor-to-sinus distance measurement for each tumor and for each reader. Thus, we used the tumor-to-sinus distance measurements obtained from the transverse imaging plane in 86% (157 of 183) of cases and the one obtained from the coronal imaging plane in 14% (26 of 183) of cases. The tumor-to-sinus distance was significantly shorter in cases with MVBI (both readers: median, 0 mm; range, 0–0 mm) than in cases without MVBI (reader 1: median, 0 mm, range, 0–16 mm; reader 2: median, 0 mm, range, 0–13 mm; $P < .001$).

In all cases with a tumor-to-sinus distance greater than 0 mm ($n = 49$), MVBI was absent at histopathologic examination. In all cases with evidence of renal sinus fat invasion at imaging ($n = 48$), MVBI was present at histopathologic examination. MVBI was present in 21% (18 of 86) of cases in which renal sinus fat invasion was absent at imaging and the tumor-to-sinus distance was 0 mm. In patients without evidence of renal sinus fat invasion at imaging ($n = 135$), a tumor-to-sinus distance of 0 mm had a sensitivity, specificity, negative predictive value, and positive predictive value for the detection of MVBI of 100% (95% CI: 81%, 100%), 42% (95% CI: 33%, 51%), 100% (95% CI: 93%, 100%), and 21% (95% CI: 13%, 31%), respectively (18 true-positive, 49 true-negative, 68 false-positive, and no false-negative findings).

Discussion

In patients with RCC, MVBI is an important prognostic parameter regarding recurrence-free and overall survival and a TNM stage-defining criterion. Our study yielded three key findings. First, all patients with evidence of renal sinus fat invasion at T2-weighted MR imaging had MVBI at histopathologic examination. Second, MVBI was found at histopathologic examination in 21% (18 of 86) of patients who had no

evidence of renal sinus fat invasion at imaging and a tumor-to-sinus distance of 0 mm. Third, in patients without evidence of renal sinus fat invasion at imaging, a tumor-to-sinus distance of 0 mm had sensitivity and specificity for the detection of MVBI of 100% and 42%, respectively.

Although none of the patients with a tumor-to-sinus distance greater than 0 mm had MVBI, our data indicate that the shorter the tumor-to-sinus distance, the higher the likelihood of MVBI. Thus, the tumor-to-sinus distance should be measured on both the transverse and coronal imaging planes, and the shorter one should be used. In our study, measurements derived from the transverse imaging plane were shorter than the ones derived from the coronal plane in 86% (157 of 183) of cases.

MVBI was found predominantly in clear cell carcinomas, which is not surprising because clear cell carcinomas are the most aggressive type of renal cortical tumor (14). However, MVBI was not found exclusively in clear cell carcinomas but also appeared in chromophobe and unclassified carcinomas. In our study, all patients with evidence of renal sinus fat invasion at imaging had MVBI at histopathologic examination. This finding supports those of a prior histopathologic study (5) in which the investigators found that renal sinus fat invasion always occurred after MVBI.

Our results suggest that the assessment of a renal tumor's relationship to the renal sinus fat could improve the identification of patients with and—more importantly—those without MVBI. According to our findings, 21% (18 of 86) of patients in whom the renal tumor was in contact with the renal sinus (ie, the tumor-to-sinus distance was 0 mm) and who usually would be assigned a tumor stage of T2, in fact had stage T3 disease owing to the presence of MVBI. In addition, the distance between a renal tumor and the renal sinus fat could affect surgical planning. Thus, surgeons should be aware of the fact that renal tumors that are in direct contact with the renal sinus fat at

T2-weighted MR imaging have a substantially higher risk of causing MVBI than do tumors separated from the renal sinus fat. Hence, the results of this study could influence a surgeon's decision between partial and radical nephrectomy.

Our study had the following limitation. Although contrast material-enhanced MR imaging was available in most cases, we did not incorporate it in our analysis, even though it may be more accurate than T2-weighted MR imaging for outlining tumor margins. We made this decision in part because we considered it important to measure the tumor-to-sinus distance in two imaging planes (transverse and coronal) because of the kidney's anatomy and alignment in the retroperitoneal space, but contrast-enhanced MR images were available in only the transverse plane in most patients. In addition, we considered T2-weighted MR images more useful for illustrating relevant anatomic details of the renal hilum.

In summary, the relationship between a renal tumor and the renal sinus fat at T2-weighted MR imaging was associated closely with the presence or absence of MVBI at histopathologic examination. Although MVBI was identified in all tumors exhibiting renal sinus fat invasion at imaging, it also was found in one-fifth of tumors that were in contact with—but not invading—the renal sinus fat at imaging. More importantly,

a tumor-to-sinus distance of more than 0 mm could be used to rule out MVBI. In conclusion, tumor-to-sinus distance measurements and the qualitative assessment of renal sinus fat invasion at T2-weighted imaging provide useful surrogate markers to rule out MVBI reliably in patients with RCC.

Disclosures of Conflicts of Interest: C.A.K. No relevant conflicts of interest to disclose. P.L.D.P. No relevant conflicts of interest to disclose. O.F.D. No relevant conflicts of interest to disclose. P.R. Financial activities related to the present article: none to disclose. Financial activities not related to the present article: is a consultant to Willex. Other relationships: none to disclose. S.T. No relevant conflicts of interest to disclose. H.H. No relevant conflicts of interest to disclose. O.A. No relevant conflicts of interest to disclose.

References

1. da Costa WH, Moniz RR, da Cunha IW, Fonseca FP, Guimaraes GC, de Cássio Zequi S. Impact of renal vein invasion and fat invasion in pT3a renal cell carcinoma. *BJU Int* 2012;109(4):544–548.
2. Bertini R, Roscigno M, Freschi M, et al. The extent of tumour fat invasion affects survival in patients with renal cell carcinoma and venous tumour thrombosis. *BJU Int* 2011;108(6):820–824.
3. Bertini R, Roscigno M, Freschi M, et al. Renal sinus fat invasion in pT3a clear cell renal cell carcinoma affects outcomes of patients without nodal involvement or distant metastases. *J Urol* 2009;181(5):2027–2032.
4. Bonsib SM. The renal sinus is the principal invasive pathway: a prospective study of 100 renal cell carcinomas. *Am J Surg Pathol* 2004;28(12):1594–1600.
5. Bonsib SM. Renal veins and venous extension in clear cell renal cell carcinoma. *Mod Pathol* 2007;20(1):44–53.
6. Bonsib SM, Gibson D, Mhoon M, Greene GF. Renal sinus involvement in renal cell carcinomas. *Am J Surg Pathol* 2000;24(3):451–458.
7. Thompson RH, Blute ML, Krambeck AE, et al. Patients with pT1 renal cell carcinoma who die from disease after nephrectomy have unrecognized renal sinus fat invasion. *Am J Surg Pathol* 2007;31(7):1089–1093.
8. Kidney. In: Edge SB, Byrd DR, Compton CC, Fritz AG, Greene FL, Trotti A, eds. *AJCC cancer staging manual*. 7th ed. New York, NY: Springer, 2010; 479–489.
9. Feifer A, Savage C, Rayala H, et al. Prognostic impact of muscular venous branch invasion in localized renal cell carcinoma cases. *J Urol* 2011;185(1):37–42.
10. Nikken JJ, Krestin GP. MRI of the kidney: state of the art. *Eur Radiol* 2007;17(11):2780–2793.
11. Greene FL, Page DL, Fleming ID, et al. *AJCC cancer staging manual*. 6th ed. New York, NY: Springer-Verlag, 2002.
12. Fuhrman SA, Lasky LC, Limas C. Prognostic significance of morphologic parameters in renal cell carcinoma. *Am J Surg Pathol* 1982;6(7):655–663.
13. Shrout PE, Fleiss JL. Intraclass correlations: uses in assessing rater reliability. *Psychol Bull* 1979;86(2):420–428.
14. Sun M, Lughezzani G, Jeldres C, et al. A proposal for reclassification of the Fuhrman grading system in patients with clear cell renal cell carcinoma. *Eur Urol* 2009;56(5):775–781.